Journal of Translational Medicine

RESEARCH

Open Access

Combining functional and morphological retinal vascular characteristics achieves high-precision diagnosis of mild non-proliferative diabetic retinopathy

Jinze Zhang[1†], Ke Ma[1,2†], Zhongzhou Luo[1], Gengyuan Wang[1], Ziqing Feng[1], Yuancong Huang[1], Keyi Fei[1], Yushuang Liu[1], Honghui Xia[3], Jin Yuan[1*] and Peng Xiao[1*]

Abstract

Background To explore the functional and morphological variations of retinal vessels in diabetes with no clinically detectable retinopathy (NDR) and mild non-proliferative diabetic retinopathy (NPDR) and to establish a high-performance mild NPDR diagnostic model.

Methods Normal subjects and type 2 diabetes patients with NDR and mild NPDR were recruited. Oxygen-saturation-related functional parameter (optical density ratio ODR) and morphological characteristics (fractal dimension D_f, vessel area rate VAR, mean vascular diameter D_m, vessel tortuosity τ) of different vascular areas were extracted with single fundus photography and comprehensively analyzed among groups. An interpretable model combining marine predator algorithm (MPA) and support vector machine (SVM) based on characteristic selection was proposed for mild NPDR diagnosis.

Results A total of 91 NDR subjects, 75 mild NPDR subjects, and 111 sex- and age-matched normal controls were analyzed. Increased main vessels ODR, while lower VAR of all areas except outer ring macula, lower D_m of all vessels and decreased τ of all areas were associate with NDR (e.g. main vessels ODR: OR [95%CI] 1.42[1.07–1.89], full macula τ:0.53[0.38–0.74]). Increased ODR of all areas, higher D_m of all areas except inner ring macula, increased inner ring macula τ, while decreased D_f of full and inner ring macula, lower VAR of all areas were associate with mild NPDR (e.g. main vessels ODR:5.68[3.03–10.65], inner ring macula VAR: 0.48[0.33–0.69]). The MPA-SVM model with selected characteristics obtained the best diagnosis performance (AUC:0.940 ± 0.014; Accuracy:90.4 ± 3.9%; Sensitivity:89.2 ± 6.4%; Specificity:91.3 ± 6.4%).

†Jinze Zhang and Ke Ma contributed equally to this work.

*Correspondence:
Jin Yuan
yuanjincornea@126.com
Peng Xiao
xiaopengaddis@hotmail.com

Full list of author information is available at the end of the article

Conclusions More significant retinal vascular variations are associate with the incidence of mild NPDR than NDR. High-precision mild NPDR diagnosis is achieved combining the morphological and functional vascular characteristics based on characteristic selection.

Keywords Diabetic retinopathy, Retinal vascular characteristics, Diagnosis modelling, Fundus photography

Introduction

Based on data from the International Diabetes Federation (IDF), approximately 540 million people of working age worldwide have diabetes (DM) in 2021, and that number will rise to 780 million by 2045 [1]. Diabetic Retinopathy (DR) is the most common complication of diabetes, affecting at least one-third of the population with DM, and can lead to blindness [2]. DR is divided into mild non-proliferative diabetic retinopathy (NPDR), which only shows fundus microaneurysms in the early stage, and progresses to moderate and severe NPDR with the increase of microaneurysms and hemorrhage. Once neovascularization or vitreous hemorrhage occurs, it is considered as proliferative diabetic retinopathy (PDR), and fundus photographs are utilized as a standard imaging modality for this grading [3, 4]. Thus, fundus screening is among the vital measures in the health management of millions of people with DM since early detection and timely treatment of DR can potentially prevent approximately 95% of DR-induced blindness [5].

However, the large population of DM patients and the uneven distribution of medical resources, especially the lack of qualified image graders, have posed great challenges for large-scale DR screening. This situation started to be ameliorated with the clinical application of artificial intelligence (AI) [6]. Nowadays, various groups have adopted machine learning or deep learning algorithms in fundus image analysis for automated DR diagnosis and grading, some of which have already been officially approved for commercial use (such as iDx-DR in the USA, Airdoc in China, Retmarker DR in the EU, etc.) [7, 8]. While the published robust diagnostic performance of these AI-assisted DR detection systems are comparable to medical experts with claimed sensitivity up to 90%, they are mostly limited to detecting moderate and severe NPDR and diabetic maculopathy, but either fail or have low sensitivity of less than 80% when diagnosing mild NPDR [9]. This is mainly due to the fact that most of the feature-based algorithms focus on detecting DR lesions, while these changes are rarely apparent in mild NPDR [10].

Vascular endothelial dysfunction and hyperglycemia caused by DM are critical factors of diabetic vascular complications, which can lead to the early and persistent changes in the morphology and function of blood vessels [11]. With the help of the self-developed retinal vascular intelligent analysis system, our team proposed the optical density ratio (ODR), a parameter related to blood oxygen function [12], and a variety of quantitative vascular morphological features, such as fractal dimension, tortuosity, vessel diameter, etc. have been proposed [13, 14]. Our previous results show that significant changes in blood oxygen function and morphological characteristics have occurred in DM patients without clinical retinopathy [12, 13]. Other observational prospective cohort studies have also concluded that abnormal changes of retinal vascular tortuosity and fractal dimension are significantly related to the progression of DR [15, 16]. Meanwhile, hyperglycemia of DM has been proven to affect retinal autoregulatory with increased blood flow and substantially increased retinal oxygen consumption [17]. Several coherent studies have further evaluated the retinal blood oxygen saturation, which can be measured with fundus oximetry, as one of the main functional changes in DM patients and during DR progression [18, 19]. Thus, jointly characterizing the detailed functional and morphological changes in retinal blood vessels, which take place in diabetes long before detectable DR lesions exist, would potentially offer an alternative approach for more precise early DR detection compared to lesion-based AI-assisted systems.

In this study, we used fundus images to fully explore the functional and morphological changes of retinal vessels in diabetic and mild NPDR, and to establish a high-performance early DR diagnostic model combining retinal vascular morphological and functional characteristics. Solely based on one traditional fundus image, both the structural and oxygen saturation-related functional variations of the subject's retinal vascular network were quantified using a customized retinal vasculature analysis system. The characteristics of retinal vessels in normal control group and diabetic groups, including no-clinically detectable retinopathy (NDR) and mild NPDR were comprehensively analyzed. An interpretable mild NPDR diagnosis method was further proposed combining the marine predator algorithm (MPA) and a machine learning algorithm for optimal characteristic subset selection and diagnosis modeling among the retinal vascular characteristics.

Methods

Participants

This is a retrospective multicenter study with participants from Zhongshan Ophthalmic Center, Guangzhou, China, and 13 community hospitals in Zhaoqing City, Guangdong, China between 1 Jan. 2019 and 15 May 2021. The

study has been approved by the Ethics Committee of Zhongshan Ophthalmic Center, Sun Yat-sen University (protocol number: 2017KYPJ104) and all procedures were in line with the Helsinki Declaration.

This study has included 166 diabetic participants (91 with NDR and 75 with mild NPDR) who met the diabetes diagnostic criteria of the American Diabetes Association [20], and 111 healthy normal subjects matched in age and sex. All participants have undergone standardized ophthalmological examinations and a detailed medical history screening. A commercial fundus camera (RetiCam 3100, SYSEYE, China) was used to capture color fundus photography. The classification of NDR and mild NPDR is derived from case system records. Images with poor image quality due to refractive media turbidity were excluded. Patients with more than moderate NPDR, PDR, diabetic macular edema (DME), other ocular diseases, infections or trauma were also ruled out. Systemic diseases that may affect oxygen saturation, such as hypertension and pulmonary disease, were also excluded. The above exclusion criteria are also applicable to normal group.

Measurement of retinal vascular morphological and functional characteristics

To obtain the quantitative functional and morphological characteristics of the retinal vascular network, the acquired fundus photograph of each subject centered on the macula was selected and analyzed by our self-developed semi-automatic retinal vascular analysis system. Details of the image processing procedures and parameter extraction can be referred to our former publications [12–14]. In brief, as shown in Fig. 1, the fundus photos are first processed by the deep learning algorithm, multi-path recurrent U-Net network [21], to extract the binarized vascular network (Fig. 1B), and the morphological characteristics in the ETDRS area (Fig. 1C) are analyzed. Then, the oxygen-sensitive and oxygen-insensitive channels corresponding to the red and green channels of fundus photography (Fig. 1D, E) are separated, and the obtained binary retinal vascular network is then combined for further analysis of the retinal vascular blood oxygen function information.

Morphological characteristics analysis module: First, we used the multi-path recurrent U-Net network for vascular network segmentation. Based on the segmented vascular network and the ETDRS area, morphological characteristics of the vessels were calculated, including fractional dimension (D_f), vessel area ratio (VAR), mean vessel diameter (D_m) and tortuosity (τ), more details of which can be found in our previous publications [13, 14]. D_f is a statistic value of space-filling fractal degree calculated with vessel skeletons, describing the vascular network complexity. VAR is the area ratio of the vascular region in the region of interest (ROI). D_m is the average diameter of all vessels in the ROI. And τ is a variable used to describe the tortuosity of the segmented blood vessels. The abovementioned morphological characteristics were calculated for all vessels of the segmented retinal vascular network, as well as for the full macula area (6 mm diameter circle centered at the fovea center), the outer ring (3–6 mm ring around the fovea) and the inner ring (1–3 mm ring around the fovea) macula areas respectively, referring to the ETDRS grid standard [22]. The innermost circle around the fovea is excluded for this analysis as the central macular area has very few visible vessels in fundus photographs.

Functional characteristics analysis module: Based on the differences in absorption of light of different wavelengths between oxygenated and deoxygenated hemoglobin in blood [23], we calculated the oxygen-saturation-related functional parameter, optical density ratio (ODR), of retinal blood vessels with only one color fundus image [12]. This is achieved by extracting the red and green channels of the color fundus photograph, representing the oxygen-sensitive and oxygen-insensitive signals respectively. ODR is linearly correlated with blood oxygen saturation [24, 25], defined as $ODR = OD_{red}/OD_{green}$, where OD is the optical density of the retinal vessels, calculated as the logarithm of the inner and outer gray values of the segmented retinal vessels in the extracted green and red image channels. Through the superposition analysis of the binary retinal vascular network with the morphological feature analysis module, the ODR values of all blood vessels, main vessels and micro vessels were extracted. Referring to the retinal oximetry, the main vessels and micro vessels are distinguished by the diameter of 6 pixels (1pixel ≈ 12.69 μm in this study) [26].

Statistical analysis

To avoid the influence of binocular interaction, each patient's macula-centered fundus color photograph from one eye was randomly selected for analysis. A Kolmogorov-Smirnov test was conducted to assess the normality of the data. Differences between groups were compared using one-way analysis of variance (ANOVA) or Kruskal-Wallis test or chi-square test. All *p*-values were corrected using the Bonferroni's post-hoc test. All data were standardized. Univariate logistic regression analysis was used for their association with NDR and mild NPDR. The odds ratio (OR) and its 95% confidence interval (CI) per 1-SD increase for each parameter were calculated to measure the level of association. A *p*-value of less than 0.05 was considered significant. Statistical analysis was performed using SPSS 25.0 (SPSS Inc., Chicago, IL, USA).

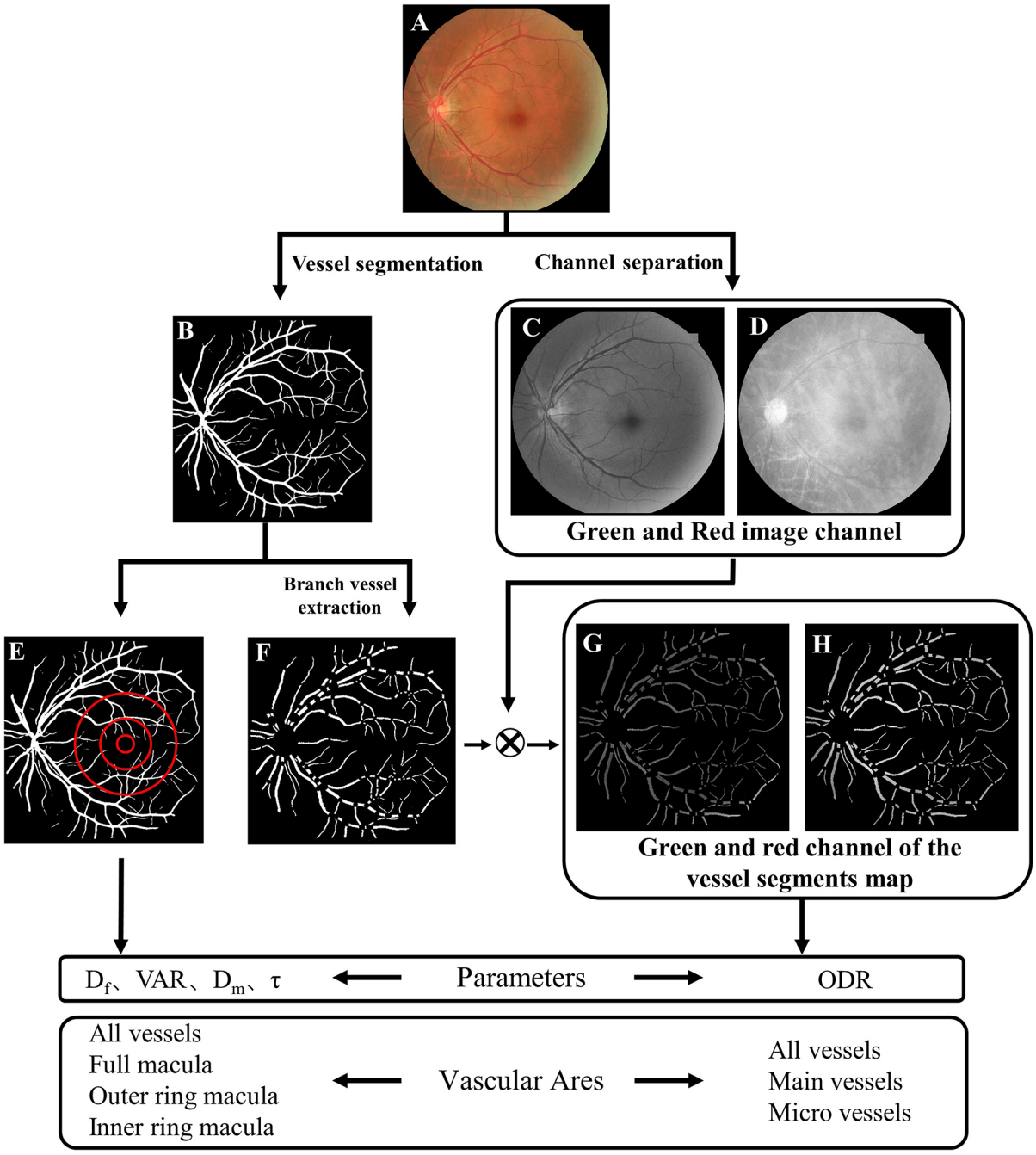

Fig. 1 Image processing procedures. (**A**) Fundus photography (**B**) Binarized vascular network. **C** and **D**. Oxygen-sensitive and oxygen-insensitive signals. **E**. ETDRS area of binary retinal vascular network. **F**. Retinal vessel segments map. **G** and **H**. Oxygen-sensitive and oxygen-insensitive channel of the vessel segments map

Interpretable mild NPDR diagnosis modeling

The above calculated functional (3 characteristics) and morphological (16 characteristics) characteristics of the retinal vascular network were fused to form the all characteristics group (19 characteristics in total) for high-precision mild NPDR diagnosis modeling. For this purpose, we applied an efficient method combining the marine predator algorithm (MPA), a metaheuristic algorithm with strong search performance for optimal characteristics selection among the fused characteristic, and a machine learning algorithm for distinguishing between NDR and mild NPDR. Specifically, MPA was used for searching characteristics subset and hyper characteristics of the machine learning algorithm, while the machine

learning algorithm was used for classification, and its categorization error is used to construct the fitness function of MPA, thus simultaneously achieving the screening of fused characteristics, optimization of hyper characteristics and mild NPDR diagnosis. Details of the modeling method implementation of MPA and machine learning can be referred to our previous publication [27]. In this manuscript, the support vector machine (SVM) with two hyper characteristics (penalty factor and bandwidth of radial basis function kernel) was applied as the machine learning algorithm in the modeling process. A five-fold cross-validation approach was applied to reliably assess model performance, using accuracy, sensitivity, specificity and mean area under the receiver operating curve (AUC) as model evaluation metrics. During the iteration of feature selection and classification algorithms, the diagnostic model was analyzed and automatically ranked for 100 different feature combinations. The best model, determined by the highest accuracy, was selected as the final diagnostic performance. To validate the effectiveness of combining functional and morphological characteristics as well as the proposed algorithm of optimal feature selection for mild NPDR diagnosis modeling, we have compared the mild NPDR diagnosis model performance based on the optimal selected characteristics to that based on three different parameter groups, i.e. functional, morphological and all characteristics without feature selection. The modeling process of these three parameter groups were set the same except that no characteristic parameter selection procedure was performed. Specifically, the hyper characteristics of the classifier with better classification performance were optimized using MPA, and then this classifier was used for mild NPDR diagnosis with the same abovementioned performance validation method and evaluation metrics. To investigate the effect of the selected characteristics of the best mild NPDR diagnosis model, a global interpretability investigation was conducted by using SHapley Additive exPlanations (SHAP), a weighted explanatory method inspired by Shapley values based on game theory [28], giving the feature importance and contribution ranking of all the selected characteristics. Specifically, SHAP computes an importance factor for each characteristic based on Shapley values to quantify the influence of that characteristic on a prediction, which is not model-specific and therefore can explain the results of any black-box model such as the SVM. Hence, we used the SHAP library in Python to achieve explainability of the mild NPDR diagnostic model. Given that five models were built in the five-fold cross-validation, we interpreted the classification model with the best classification performance. The optimal SVM model was explained using the kernel interpreter in the SHAP library and using the summary plot of SHAP to display the significance of all characteristics.

Table 1 Basic clinical information of participants

	Normal	DM		p^a
		NDR	mild NPDR	
No, of subjects	111	91	75	
Age, yrs. Mean (SD)	48.38(7.71)	48.60(10.36)	50.64(8.59)	0.581
Median (Rang)	48.00 (35–65)	49.00 (33–63)	51.00 (30–70)	
Sex, Male: Female	55:56	48:43	43:32	0.579
Blood glucose, mmol/l. Mean (SD)	-	8.89(4.55)	9.56(4.17)	NA
Median (Rang)		7.30 (3.98–25.9)	8.30 (3.50–31.60)	

a: ANOVA or chi-square test between all groups. DM, diabetes mellitus; NDR, no clinically detectable retinopathy; mild NPDR, non-proliferative diabetic retinopathy; NA, not applicable

Software

Retinal vascular analysis system was implemented with Pytorch. Image processing and analysis algorithm of the system were developed based on Python 3.6 (Python Software Foundation, Hampton, NH) with cv2 library. The MPA-SVM algorithm for characteristic selection and classification was run in Matlab 2022a (MathWorks Inc., Natick, MA, USA). Finally, the interpretable mild NPDR diagnosis model was built on Python 3.6(Python Software Foundation, Hampton, NH) with the SHAP library. The image processor was a 2 18-core Intel Xeon Processor E5-2695 v4 2.10 GHz, 128 GB memory ECC REG DDR4, 2400 MHz, 480 G 2.5-inch 6Gb enterprise-class SSD; it supports heterogeneous accelerated parallel computing and has a GPU computing power of 4×4.7 trillion times per second.

Results

There was no significant difference in age and sex between the NDR group (n=91, mean [SD] age 48.6 [10.4] years, 43 [47.3%] female) and mild NPDR group (75, 50.6 [8.6], 32 [42.3%] female) and the healthy normal group (111, 48.4 [7.7], 56 [50.5%] female). More details about clinical information of participants are shown in Table 1.

Analysis of retinal vascular characteristics among groups

The statistical comparison of the retinal vascular network characteristics of different analyzed vascular areas among groups are shown in Fig. 2. The specific characteristics and corrected p values can be referred to the Supplementary Table 1. From Normal to NDR and then to mild NPDR group, the functional parameter ODR of all vessels, main and micro vessels showed an increasing trend continuously. All ODR were significantly greater (p<0.001, respectively) in mild NPDR compared to Normal group as well as NDR group, while the main vessels ODR was greater (p<0.05) in NDR group compared to Normal group significantly. The morphological

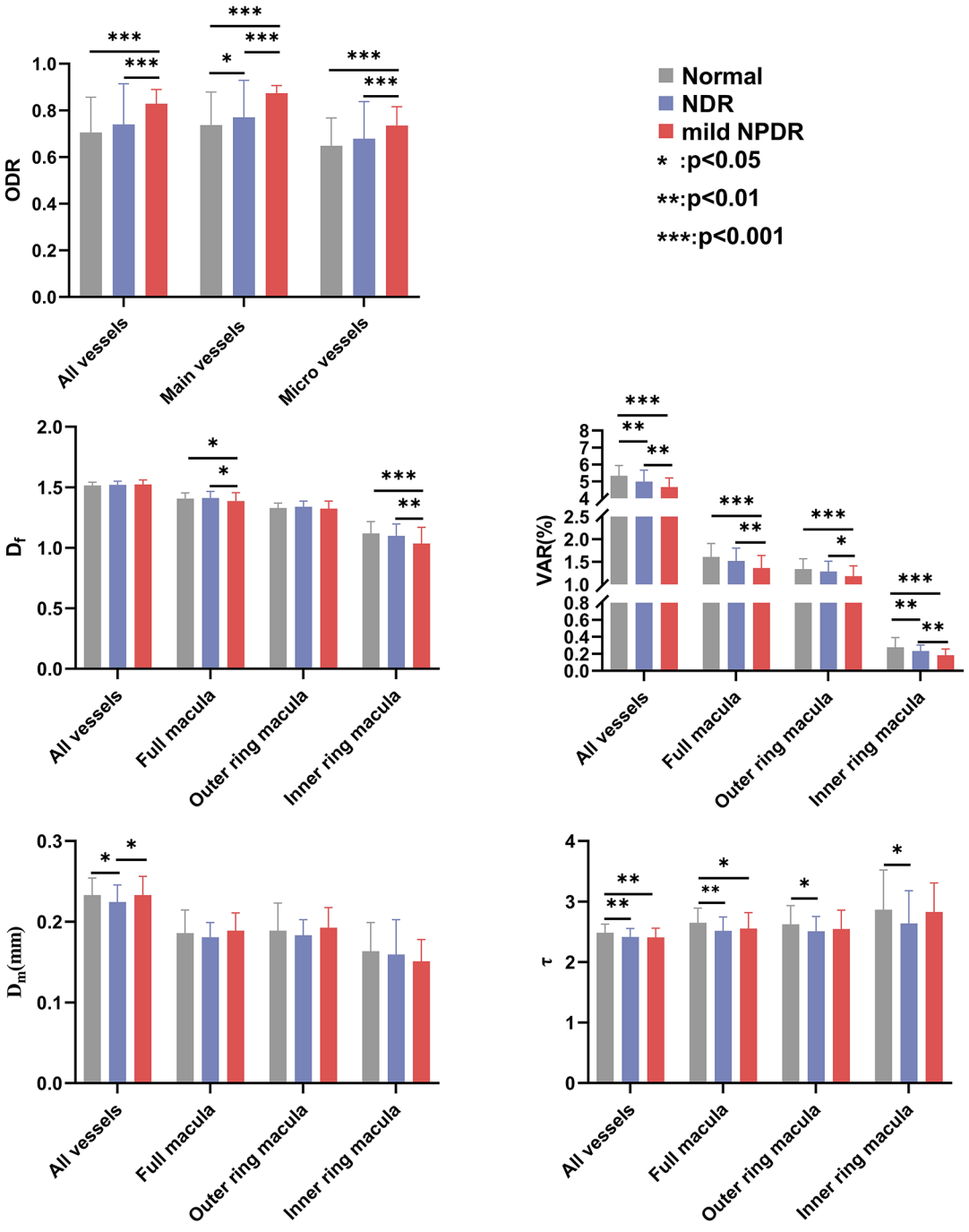

Fig. 2 Statistical comparison of retinal vascular characteristics among the Normal, NDR and mild NPDR groups. ODR histograms represent the median, and error bars indicate the interquartile range (IQR), the other histograms represent the average and error bars indicate standard deviation (SD). NDR, no clinically detectable retinopathy; mild NPDR, non-proliferative diabetic retinopathy; ODR, optical density ratio; D_f, fractal dimension; VAR, vessel area rate; D_m, mean vascular diameter; τ, vessel tortuosity

characteristics showed more diverse changes. D_f of both the full macula and inner ring macula in mild NPDR group were lower compared to that in Normal ($p<0.05$, respectively) and NDR ($p<0.05$, respectively) group. VAR showed a decline trend from Normal to NDR and then to mild NPDR group. In the mild NPDR group, VAR of all the vascular areas were significantly lower compared to both Normal group ($p<0.001$, respectively) and NDR group ($p<0.05$, respectively). In the NDR group, VAR of all vessels and inner ring macula were significantly lower ($p<0.01$, respectively) compared to the Normal group. The difference of D_m was mainly manifested in all vessels,

Table 2 Association between retinal vascular characteristics and the incidence of NDR and mild NPDR

	Normal-NDR		NDR-mild NPDR	
	OR (95% CI)	*P* value	OR (95% CI)	*P* value
Optical density ratio, ODR				
All vessels	1.24 (0.93–1.63)	0.138	3.40 (2.16–5.36)	< 0.001*
Main vessels	1.42 (1.07–1.89)	0.016*	5.68 (3.03–10.65)	< 0.001*
Micro vessels	1.13 (0.85–1.49)	0.405	2.51 (1.69–3.74)	< 0.001*
Fractal dimension, D_f				
All vessels	1.23 (0.93–1.63)	0.156	1.12 (0.82–1.52)	0.470
Full macula	1.11 (0.84–1.46)	0.478	0.65 (0.47–0.90)	0.006*
Outer ring macula	1.23 (0.93–1.63)	0.155	0.77 (0.56–1.05)	0.097
Inner ring macula	0.82 (0.62–1.08)	0.158	0.56 (0.40–0.79)	0.001*
Vessel area rate, VAR				
All vessels	0.57 (0.42–0.78)	< 0.001*	0.57 (0.41–0.80)	0.001*
Full macula	0.73 (0.55–0.97)	0.032*	0.56 (0.40–0.78)	0.001*
Outer ring macula	0.79 (0.60–1.05)	0.110	0.63 (0.45–0.88)	0.006*
Inner ring macula	0.57 (0.40–0.81)	0.002*	0.48 (0.33–0.69)	< 0.001*
Mean vascular diameter, D_m				
All vessels	0.66(0.49–0.89)	0.006*	1.49 (1.08–2.05)	0.016*
Full macula	0.77 (0.55–1.09)	0.145	1.52 (1.09–2.12)	0.013*
Outer ring macula	0.78 (0.54–1.12)	0.178	1.57 (1.12–2.21)	0.009*
Inner ring macula	0.90 (0.68–1.19)	0.464	0.79 (0.56–1.10)	0.154
Vessel tortuosity, τ				
All vessels	0.58(0.43–0.80)	0.001*	0.96 (0.70–1.30)	0.774
Full macula	0.53(0.38–0.74)	< 0.001*	1.17 (0.86–1.59)	0.313
Outer ring macula	0.64 (0.47–0.88)	0.006*	1.16 (0.84–1.59)	0.373
Inner ring macula	0.66 (0.47–0.91)	0.011*	1.49 (1.05–2.10)	0.024*

Univariates logistic regression of the associations between the retinal vascular characteristics and the incidence of NDR and mild NPDR with age and sex adjusted.

*: $p < 0.05$.

it was significantly lower ($p < 0.05$) in NDR group compared to Normal group, but significantly higher ($p < 0.05$) in mild NPDR compared to NDR group. τ of all areas were significantly lower ($p < 0.05$, respectively) in NDR group compared to Normal group, while it of the full vessels and full macula were significant lower ($p < 0.05$, respectively) in mild NPDR group compared to Normal group.

Correlation of retinal vascular characteristics with the incidence of NDR and mild NPDR

Table 2 presents the results of univariate logistic regression, indicating the relationships between retinal vascular characteristics and the incidence of NDR compared to the Normal group, as well as mild NPDR compared to the NDR group. Generally, more retinal vascular characteristics were found to be associated with the incidence of mild NPDR compared to NDR. Increased main vessels ODR (OR, 1.42; 95%CI, [1.07–1.89]; $p = 0.016$), decreased VAR of all areas except the outer ring macula (e.g. inner ring macula: 0.57; [0.40–0.81]; $p < 0.001$), smaller all vessels D_m (0.66; [0.49–0.89]; $p = 0.006$), and decreased τ of all areas (e.g. full macula: 0.53; [0.38–0.74]; $p < 0.001$) were found to have significant associations with the incidence of NDR. While increased ODR of all areas (e.g. main vessels: 5.68; [3.03–10.65]; $p < 0.001$), larger D_m of all areas except the inner ring macula (e.g. outer ring macula: 1.57; [1.12–2.21]; $p = 0.009$), greater inner ring macula τ (1.49; [1.05–2.10]; 0 = 0.024), decreased D_f of full macula (OR, 0.65; [0.47–0.90]; $p = 0.006$) and inner ring macula (0.56; [0.40–0.79]; $p = 0.001$), lower VAR of all areas (e.g. inner ring macula: 0.48; [0.33–0.69]; $p < 0.001$) were found significantly associated with the presence of mild NPDR.

Table 3 The diagnosis performance of mild NPDR with different parameter combinations

Modeling characteristics	Accuracy	Sensitivity	Specificity
Morphological characteristics	76.5 ± 3.1%	70.3 ± 14.0%	81.4 ± 12.8%
Functional characteristics	78.3 ± 5.8%	80.9 ± 14.8%	76.1 ± 11.0%
All characteristics	85.5 ± 1.3%	82.7 ± 7.9%	88.1 ± 6.4%
Selected characteristics	**90.4 ± 3.9%**	**89.2 ± 6.4%**	**91.3 ± 6.4%**

Reliable evaluation of model performance by applying a five-fold cross-validation approach

Performances of mild NPDR diagnosis models based on retinal vascular characteristics

The classification results of 100 repeated runs of MPA-SVM are shown in Supplementary Table 2. The modeling result with the highest average accuracy was selected as the final diagnostic performance of the mild NPDR diagnosis. As shown in Table 3; Fig. 3a, the MPA-SVM modeling of mild NPDR diagnosis demonstrated better performance based on the functional retinal vascular characteristics (3 parameters, AUC: 0.863 ± 0.071; accuracy: 78.3 ± 5.8%; sensitivity: 80.9 ± 14.8%; specificity: 76.1 ± 11.0%) than that based on the morphological retinal vascular characteristics (16 parameters, AUC: 0.806 ± 0.030; accuracy: 76.5 ± 3.1%; sensitivity: 70.3 ± 14.0%; specificity: 81.4 ± 12.8%). Combining all the morphological and functional characteristics, the model achieved a diagnosis performance superior to that solely based on either morphological or functional characteristics (19 parameters, AUC: 0.904 ± 0.034; accuracy:85.5 ± 1.3%; sensitivity:82.7 ± 7.9%; specificity: 88.1 ± 6.4%). By performing feature selection in the MPA-SVM modeling using all the characteristics, the best mild NPDR diagnosis performance (AUC: 0.940 ± 0.014; accuracy: 90.4 ± 3.9%; sensitivity: 89.2 ± 6.4%; specificity:

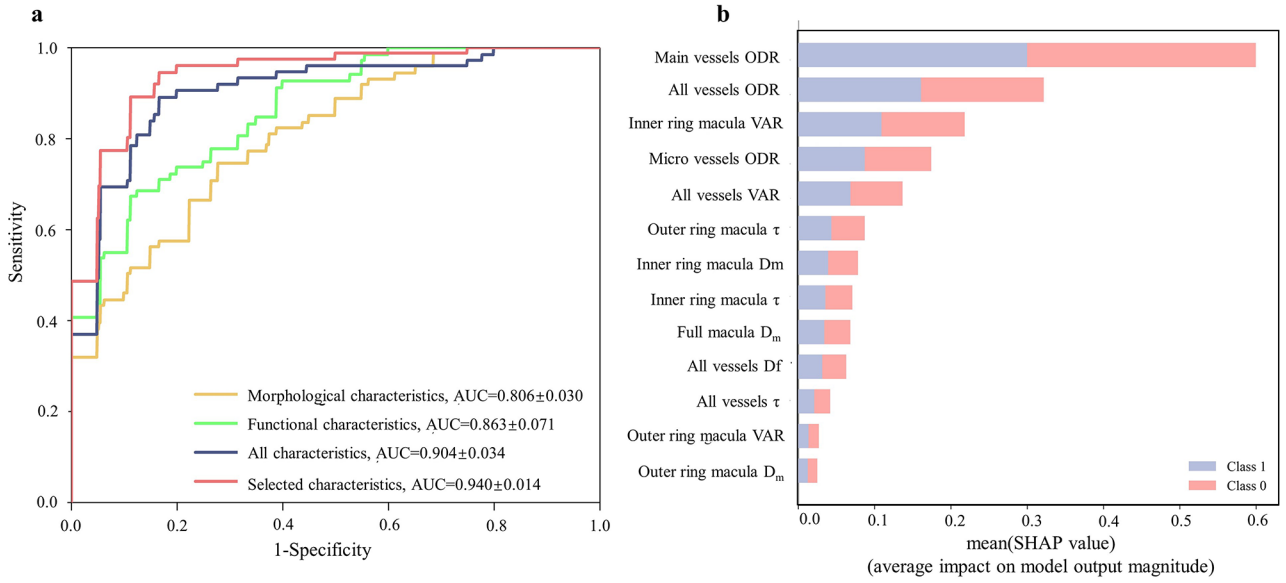

Fig. 3 (**a**) ROC curves of mild NPDR diagnosis models based on different characteristic groups. (**b**) Interpretable importance plot of the selected characteristics in the MPA-SVM model for mild NPDR diagnosis based on SHAP

91.3±6.4%) was obtained based on 13 selected functional and morphological characteristics (Fig. 3b), in which the top 5 characteristics in terms of importance were main vessels ODR, all vessels ODR, inner ring macula VAR, micro vessels ODR and all vessels VAR, containing all the three extracted functional characteristics.

Discussion

In this study of DM patients with NDR and mild NPDR, both the morphological and functional characteristics of the retinal vascular network were thoroughly extracted and quantified using a customized computational analysis system solely based on a single traditional fundus image. Retinal vascular changes were found to occur already at the stage of NDR and more retinal vascular characteristic variations, especially the oxygen-saturation-related ODRs and VARs, were found to be significantly associated with the incidence of mild NPDR rather than NDR. On this basis, we demonstrated that combining both morphological and functional retinal vascular characteristics showed improved discrimination ability of mild NPDR from NDR compared to that based on either morphological or functional characteristics. An interpretable high-performance mild NPDR diagnosis model was further established based on the feature selection among the morphological and functional retinal vascular characteristics. Our findings offer a new path of precise early DR screening with the concept of computational retinal vascular network assessment in fundus photographs.

The comprehensive analysis results of retinal vascular changes in NDR and mild NPDR revealed that the functional parameter ODRs mainly showed a sustained increase with a more significant increase observed in mild NPDR compared to NDR, indicating an exacerbated oxygen saturation abnormality in retinal vessels as the disease progressed. In DM patients, glycated hemoglobin has a higher oxygen binding capacity [29], which could explain the increased oxygen saturation levels in the NDR group. In addition, in patients with DR, capillary nonperfusion and shunting may lead to uneven blood flow distribution, and impaired oxygen delivery from blood to retinal tissue would further lead to additional increases in oxygen saturation [30]. The subsequent compensatory mechanisms of the body resulting from tissue hypoxia increase the oxygen supply to the retinal vessels leading to even higher oxygen saturation levels in DR. While higher retinal oxygen saturation has also been found in former studies in more severe DR stages [18, 19, 31], our results demonstrated that this alteration was already significant in mild NPDR, which might be a potential influence mechanism of early DR development, and this was supported by the more significant association between oxygen-saturation-related retinal vascular characteristics and the incidence of mild NPDR compare to NDR.

The changes of the retinal vascular morphology in NDR and mild NPDR are diversified. More alterations of vascular morphological characteristics, except vessel tortuosity, were found to be associated with the incidence of mild NPDR compared to NDR. The decrease in macular fractal dimension in mild NPDR indicates a reduced two-dimensional space-filling vascular complexity that occurs in the microvascular area already during early DR, which correlates with previous findings in DR patients with type 2 diabetes as well as type 1 diabetes

[16, 32, 33]. The direct mechanism associated with fractal dimension alteration is complex due to there are cumulative effects during the disease progression [16]. In other words, the change of fractal dimension in different stages of DR may be discontinuous, and the fractal dimension of proliferative DR characterized by neovascularization may increase. This may be the potential reason why some studies have shown contradictory results [34, 35], which requires more in-depth studies to explain. VAR showed a sustained decrease in all VARs and was more significant in mild NPDR compared to NDR. These reductions in vascular density may result from the vessel loss and the capillary non-perfusion due to the vascular hemodynamics alterations in DM patients [30]. Lee et al. demonstrated that an increased capillary non-perfusion area was associated with the occurrence of DR by fluorescein angiography [36], and the same findings were confirmed in an OCTA-based study [37]. It is worth mentioning that the changes of the vascular fractal dimension and vascular density in the inner macular ring are more obvious and significant than those in the outer macular ring, which indicates that the early morphological changes occur from microcapillaries. Significant changes in blood vessel diameter are mainly observed in all vessels in our study. Vascular endothelial dysfunction in diabetes is mainly characterized by decreased endothelium-dependent relaxation and/or enhanced endothelium-dependent contractile function, so it will lead to vasoconstriction throughout course of diabetes [38], and the vessel diameter showed a decreasing trend in NDR. However, in mild NPDR, the further increase in vascular diameter may be due to the damage of endothelium-dependent vasodilation associated with the decrease of endothelium-derived nitric oxide and/or the increase of reactive oxygen species production [39, 40]. In addition, increased retinal blood flow [41] and hyperglycemia-mediated overactivation of protein kinase Cs [42] in DR may also lead to vasodilation. The alterations of blood vessel diameter in the macula area could also occur since larger macular vessel diameter was found to be associated with the incidence of mild NPDR, but the observed differences between groups were not obvious, which may be due to the low image resolution of fundus photography. The lower vessel tortuosity observed in NDR in our study could be related to the straightening of blood vessels caused also by vasoconstriction and vascular hypoperfusion [43, 44], which is weakened in the DR stage. The increase of tortuosity in mild NPDR is related to tissue hypoxia, endothelial dysfunction and the increase of vascular endothelial growth factor [34, 45].

As a typical vascular complication of DM, the development of DR is inevitably accompanied by abnormal changes in retinal vascular functions [19, 31, 46], some of which are actually direct causes of retinal vascular morphological variations. During the process of building the diagnostic model of mild NPDR, the diagnosis performance of the model using only 3 oxygen-saturation-related functional characteristics was superior to that of the model consisting of 16 morphological characteristics, which further illustrates the irreplaceable role of oxygen-related retinal vascular functional changes in the development of mild NPDR. Combining both the morphological and functional retinal vascular characteristics resulted in improved discrimination ability of mild NPDR from NDR as compared to that based on either characteristic group. By incorporating the MPA and SVM algorithms, modeling features were selected and reduced to improve system efficiency while obtaining the best mild NPDR diagnostic performance (AUC: 0.940±0.014, accuracy: 90.4±3.9%, sensitivity: 89.2±6.4% and specificity: 91.3±6.4%). Compared with other lesion-based AI-assisted DR diagnostic methods [7, 9, 47–49], our diagnostic model is specifically designed for early DR diagnosis and achieves considerable diagnostic efficiency, while our diagnostic model uses well-defined retinal vascular characteristics, which are more interpretable and solves the "black box" problem of AI algorithms to a certain extent. Despite this, the dataset included in this study is relatively small, which may lead to overfitting and consequently affect the model's generalization capabilities. To address this limitation, a five-fold cross-validation method was employed to reduce the impact of the small dataset [50]. In future work, we plan to incorporate more data to train the system, thereby enhancing the model's generalizability.

The limitations of this study include the use of a semi-automatic analysis system with manual operation of the functional and morphological parameter modules, and the absence of differentiation between arterioles and venules in retinal vessels, which could potentially offer more detailed retinal vascular information and enable more in-depth comparisons with external sources. Fully automatic processing of retinal vascular characteristics with arteriovenous differentiation is expected in our future work. As the both the morphological characteristics and functional ODRs are extracted based on traditional color fundus photograph, they are affected by the fundus camera hardware limitations of two-dimensional imaging with insufficient depth and relative low imaging resolution. Only the larger retinal vessels in the inner retina can be resolved in fundus images and subjected to quantitative analysis, which limits the comprehensive evaluation of the retinal vascular morphological and oxygen-saturation-related functional characteristics in three-dimensions, including the macular retinal capillaries. Since OCTA provides higher imaging resolution and deeper imaging depth in three-dimensions, enabling the observation and morphological analysis of smaller and deeper layers of vascular structures, incorporating

OCTA morphological parameters along with the oxygen-saturation-related functional characteristics might achieve more sensitive and effective diagnostic performance. While consistent observation of retinal vascular changes has been confirmed across imaging modalities like fluorescein angiography and OCTA [36, 37], it might worth further exploring the correlation between retinal vascular parameters based on fundus color photography and OCTA, which may support the feasibility of using fundus color photography instead of OCTA examinations in economically underdeveloped areas to help improving the accessibility of early screening and evaluation of mild NPDR and other retinal assessment in the target population. Moreover, conducting a longitudinal study to evaluate retinal vascular characteristic variations over time would further strengthen the potential value of our methods in the early detection of DR. The analysis method proposed in this study also has a wide application prospects in other retinal vascular-related ocular and systemic diseases.

In conclusion, retinal vascular functional and morphological characteristics are thoroughly characterized solely based on one fundus photography. Retinal vascular changes are found occurred already at the stage of NDR. More significant vascular variations, especially the oxygen-saturation-related ODRs and VARs, are found associated with the incidence of mild NPDR than NDR. Joint functional and morphological retinal vascular characteristics modeling achieves better discrimination ability of mild NPDR from NDR than either characteristic group. High-precision diagnosis model is established with feature selection among all the vascular characteristics, offering a robust tool for efficient early DR diagnosis that can be used in clinical practice.

Supplementary Information

The online version contains supplementary material available at https://doi.org/10.1186/s12967-024-05597-7.

Supplementary Material 1

Supplementary Material 2

Acknowledgements

The author thanks the image collectors and image readers of 13 hospitals such as Zhaoqing Gaoyao People's Hospital for their contributions to data collection and image classification.

Authors' contributions

JZ, JY and PX: conception and design of the work. All authors: acquisition, analysis or interpretation of data for the work, drafting the work. JY and PX are the guarantors of this work and, as such, have full access to all the data in the study and take responsibility for the integrity of the data and the accuracy of the data analysis.

Funding

National Natural Science Foundation of China (Nos. 82230033 and 82271133). Department of Science and Technology of Guangdong Province (Nos. 2021TX06Y127 and 2021TQ06Y137). Basic and Applied Basic Research Foundation of Guangdong Province (No. 2022A1515011486). Fundamental Research Funds for the Central Universities, Sun Yat-sen University (24ykqb009). Fundamental Research Funds of the State Key Laboratory of Ophthalmology.The funding organization had no role in the design or conduct of this research.

Declarations

Human subjects

Human Subjects were included in this study. All procedures were conducted following the Declaration of Helsinki (1983) and were approved by the Institutional Review Board of Zhongshan Ophthalmic Center, Sun Yat-sen University (protocol number: 2017KYPJ104). This study followed the STROBE guidelines strictly. No animal subjects were used in this study.

Competing interests

The authors declare no conflicts of interest.

Author details

[1]State Key Laboratory of Ophthalmology, Zhongshan Ophthalmic Center, Guangdong Provincial Key Laboratory of Ophthalmology and Visual Science, Guangdong Provincial Clinical Research Center for Ocular Diseases, Sun Yat-sen University, Guangzhou, China
[2]Department of Health Technology and Informatics, The Hong Kong Polytechnic University, Hong Kong, China
[3]Department of Ophthalmology, Zhaoqing Gaoyao People's Hospital, Zhaoqing, China

Received: 23 October 2023 / Accepted: 10 August 2024
Published online: 28 August 2024

References

1. Sun H, Saeedi P, Karuranga S, Pinkepank M, Ogurtsova K, Duncan BB, et al. IDF Diabetes Atlas: Global, regional and country-level diabetes prevalence estimates for 2021 and projections for 2045. Diabetes Res Clin Pract. 2022;183:109119.
2. Yau JWY, Rogers SL, Kawasaki R, Lamoureux EL, Kowalski JW, Bek T, et al. Global prevalence and major risk factors of Diabetic Retinopathy. Diabetes Care. 2012;35:556–64.
3. Early Treatment Diabetic Retinopathy Study Research Group. Fundus photographic risk factors for progression of diabetic retinopathy. ETDRS report number 12. Early Treatment Diabetic Retinopathy Study Research Group. Ophthalmology. 1991;98:823–33.
4. Early Treatment Diabetic Retinopathy Study. Grading diabetic retinopathy from stereoscopic color fundus photographs–an extension of the modified Airlie House classification. ETDRS report number 10. Early Treatment Diabetic Retinopathy Study Research Group. Ophthalmology. 1991;98:786–806.
5. Vujosevic S, Aldington SJ, Silva P, Hernández C, Scanlon P, Peto T, et al. Screening for diabetic retinopathy: new perspectives and challenges. Lancet Diabetes Endocrinol. 2020;8:337–47.
6. Schmidt-Erfurth U, Sadeghipour A, Gerendas BS, Waldstein SM, Bogunović H. Artificial intelligence in retina. Prog Retin Eye Res. 2018;67:1–29.
7. Ting DSW, Cheung CY-L, Lim G, Tan GSW, Quang ND, Gan A, et al. Development and validation of a Deep Learning System for Diabetic Retinopathy and Related Eye diseases using retinal images from multiethnic populations with diabetes. JAMA. 2017;318:2211–23.
8. Wang Y, Yang J, Yang J, Zhao X, Chen Y, Yu W. Progress of artificial intelligence in diabetic retinopathy screening. Diabetes Metab Res Rev. 2021;37.
9. Gargeya R, Leng T. Automated identification of Diabetic Retinopathy using deep learning. Ophthalmology. 2017;124:962–9.
10. Cheung N, Mitchell P, Wong TY. Diabetic retinopathy. Lancet. 2010;376:124–36.
11. Avogaro A, Fadini GP. Microvascular complications in diabetes: a growing concern for cardiologists. Int J Cardiol. 2019;291:29–35.
12. Zhang J, Luo Z, Wang G, Huang Y, Fei K, Liu Y, et al. Oxygen-saturation-related functional parameter as a biomarker for diabetes mellitus—extraction method and clinical validation. Front Cell Dev Biol. 2023;11:1195873.

13. Li M, Wang G, Xia H, Feng Z, Xiao P, Yuan J. Retinal vascular geometry detection as a biomarker in diabetes mellitus. Eur J Ophthalmol. 2021;112067212110334.
14. Wang G, Li M, Yun Z, Duan Z, Ma K, Luo Z, et al. A novel multiple subdivision-based algorithm for quantitative assessment of retinal vascular tortuosity. Exp Biol Med (Maywood). 2021;246:2222–9.
15. Klein R, Lee KE, Danforth L, Tsai MY, Gangnon RE, Meuer SE, et al. The relationship of Retinal Vessel geometric characteristics to the incidence and progression of Diabetic Retinopathy. Ophthalmology. 2018;125:1784–92.
16. Forster RB, Garcia ES, Sluiman AJ, Grecian SM, McLachlan S, MacGillivray TJ, et al. Retinal venular tortuosity and fractal dimension predict incident retinopathy in adults with type 2 diabetes: the Edinburgh type 2 diabetes study. Diabetologia. 2021;64:1103–12.
17. Jørgensen CM, Hardarson SH, Bek T. The oxygen saturation in retinal vessels from diabetic patients depends on the severity and type of vision-threatening retinopathy. Acta Ophthalmol. 2014;92:34–9.
18. Jørgensen C, Bek T. Increasing oxygen saturation in larger retinal vessels after photocoagulation for diabetic retinopathy. Invest Ophthalmol Vis Sci. 2014;55:5365–9.
19. Hardarson SH, Stefánsson E. Retinal oxygen saturation is altered in diabetic retinopathy. Br J Ophthalmol. 2012;96:560–3.
20. American Diabetes Association. Diagnosis and classification of diabetes Mellitus. Diabetes Care. 2011;34:S62–9.
21. Jiang Y, Wang F, Gao J, Cao S. Multi-path recurrent U-Net segmentation of Retinal Fundus Image. Appl Sci. 2020;10:3777.
22. Kinyoun J, Barton F, Fisher M, Hubbard L, Aiello L, Ferris F. Detection of Diabetic Macular Edema. Ophthalmology. 1989;96:746–51.
23. van Kampen EJ, Zijlstra WG. Spectrophotometry of hemoglobin and hemoglobin derivatives. Adv Clin Chem. 1983;23:199–257.
24. Beach JM, Schwenzer KJ, Srinivas S, Kim D, Tiedeman JS. Oximetry of retinal vessels by dual-wavelength imaging: calibration and influence of pigmentation. J Appl Physiol. 1999;86:748–58.
25. Hammer M, Vilser W, Riemer T, Schweitzer D. Retinal vessel oximetry-calibration, compensation for vessel diameter and fundus pigmentation, and reproducibility. J Biomed Opt. 2008;13:054015.
26. Geirsdottir A, Palsson O, Hardarson SH, Olafsdottir OB, Kristjansdottir JV, Stefánsson E. Retinal vessel oxygen saturation in healthy individuals. Invest Ophthalmol Vis Sci. 2012;53:5433–42.
27. Xiao P, Ma K, Gu L, Huang Y, Zhang J, Duan Z et al. Inter-Subject Prediction of Pediatric Emergence Delirium Using Feature Selection and Classification from Spontaneous EEG Signals. SSRN Journal [Internet]. 2022 [cited 2022 Sep 23]; https://www.ssrn.com/abstract=4188414
28. Lundberg S, Lee S-IA, Unified Approach to Interpreting Model Predictions. Long Beach, California, USA: arXiv; 2017 [cited 2022 Oct 22]. pp. 4768–77. http://arxiv.org/abs/1705.07874
29. Graham JJ, Ryall RG, Wise PH. Glycosylated haemoglobin and relative polycythaemia in diabetes mellitus. Diabetologia. 1980;18:205–7.
30. Cogan DG, Kuwabara T. Capillary shunts in the pathogenesis of Diabetic Retinopathy. Diabetes. 1963;12:293–300.
31. Khoobehi B, Firn K, Thompson H, Reinoso M, Beach J. Retinal arterial and venous oxygen saturation is altered in Diabetic patients. Invest Ophthalmol Vis Sci. 2013;54:7103.
32. Grauslund J, Green A, Kawasaki R, Hodgson L, Sjølie AK, Wong TY. Retinal vascular fractals and microvascular and macrovascular complications in type 1 diabetes. Ophthalmology. 2010;117:1400–5.
33. Broe R, Rasmussen ML, Frydkjaer-Olsen U, Olsen BS, Mortensen HB, Hodgson L, et al. Retinal vessel calibers predict long-term Microvascular complications in Type 1 diabetes: the Danish cohort of Pediatric Diabetes 1987 (DCPD1987). Diabetes. 2014;63:3906–14.
34. Cheung CY, Sabanayagam C, Law AK, Kumari N, Ting DS, Tan G, et al. Retinal vascular geometry and 6 year incidence and progression of diabetic retinopathy. Diabetologia. 2017;60:1770–81.
35. Lim SW, Cheung N, Wang JJ, Donaghue KC, Liew G, Islam FMA, et al. Retinal vascular fractal dimension and risk of early diabetic retinopathy: a prospective study of children and adolescents with type 1 diabetes. Diabetes Care. 2009;32:2081–3.
36. Lee WJ, Sobrin L, Kang MH, Seong M, Kim YJ, Yi J-H, et al. Ischemic diabetic retinopathy as a possible prognostic factor for chronic kidney disease progression. Eye (Lond). 2014;28:1119–25.
37. Wang Q, Liu L, Jonas JB, Gao B, Wu SL, Chen SH, et al. Albuminuria and retinal vessel density in diabetes without diabetic retinopathy: the Kailuan Eye Study. Acta Ophthalmol. 2021;99:e669–78.
38. Shi Y, Vanhoutte PM. Reactive oxygen-derived free radicals are key to the endothelial dysfunction of diabetes. J Diabetes. 2009;1:151–62.
39. Shi Y, Vanhoutte PM. Macro- and microvascular endothelial dysfunction in diabetes. J Diabetes. 2017;9:434–49.
40. Triggle CR, Ding H, Anderson TJ, Pannirselvam M. The endothelium in health and disease: a discussion of the contribution of non-nitric oxide endothelium-derived vasoactive mediators to vascular homeostasis in normal vessels and in type II diabetes. Mol Cell Biochem. 2004;263:21–7.
41. Schmetterer L, Wolzt M. Ocular blood flow and associated functional deviations in diabetic retinopathy. Diabetologia. 1999;42:387–405.
42. Curtis TM, Scholfield CN. The role of lipids and protein kinase cs in the pathogenesis of diabetic retinopathy. Diabetes Metab Res Rev. 2004;20:28–43.
43. Kohner EM, Patel V, Rassam SM. Role of blood flow and impaired autoregulation in the pathogenesis of diabetic retinopathy. Diabetes. 1995;44:603–7.
44. Owen CG, Newsom RSB, Rudnicka AR, Barman SA, Woodward EG, Ellis TJ. Diabetes and the Tortuosity of vessels of the Bulbar Conjunctiva. Ophthalmology. 2008;115:e27–32.
45. Sasongko MB, Wong TY, Nguyen TT, Cheung CY, Shaw JE, Wang JJ. Retinal vascular tortuosity in persons with diabetes and diabetic retinopathy. Diabetologia. 2011;54:2409–16.
46. Kang Q, Yang C. Oxidative stress and diabetic retinopathy: molecular mechanisms, pathogenetic role and therapeutic implications. Redox Biol. 2020;37:101799.
47. Abràmoff MD, Lou Y, Erginay A, Clarida W, Amelon R, Folk JC, et al. Improved Automated Detection of Diabetic Retinopathy on a publicly available dataset through integration of Deep Learning. Invest Ophthalmol Vis Sci. 2016;57:5200–6.
48. Bhardwaj C, Jain S, Sood M. Deep learning-based Diabetic Retinopathy Severity Grading System employing Quadrant Ensemble Model. J Digit Imaging. 2021;34:440–57.
49. Wang Y, Yu M, Hu B, Jin X, Li Y, Zhang X, et al. Deep learning-based detection and stage grading for optimising diagnosis of diabetic retinopathy. Diabetes Metab Res Rev. 2021;37:e3445.
50. Choi MY, Ma C. Making a big impact with small datasets using machine-learning approaches. Lancet Rheumatol. 2020;2:e451–2.

Publisher's Note